

Article

**External Electric Field Effects on Absorption, Fluorescence and Phosphorescence Spectra of 4-(Dimethylamino)benzonitrile in a Polymer Film**

Tomokazu Yoshizawa, Yuji Iwaki, Naoki Osaka, Takakazu Nakabayashi, Klaas A. Zachariasse, and Nobuhiro Ohta

*J. Phys. Chem. B*, **2004**, 108 (50), 19132-19139 • DOI: 10.1021/jp040012x • Publication Date (Web): 19 November 2004

Downloaded from <http://pubs.acs.org> on May 18, 2009

**More About This Article**

Additional resources and features associated with this article are available within the HTML version:

- Supporting Information
- Links to the 1 articles that cite this article, as of the time of this article download
- Access to high resolution figures
- Links to articles and content related to this article
- Copyright permission to reproduce figures and/or text from this article

[View the Full Text HTML](#)

# External Electric Field Effects on Absorption, Fluorescence and Phosphorescence Spectra of 4-(Dimethylamino)benzonitrile in a Polymer Film

Tomokazu Yoshizawa,<sup>†,‡</sup> Yuji Iwaki,<sup>†</sup> Naoki Osaka,<sup>†</sup> Takakazu Nakabayashi,<sup>†,‡</sup>  
Klaas A. Zachariasse,<sup>§</sup> and Nobuhiro Ohta<sup>\*,†,‡</sup>

Research Institute for Electronic Science (RIES), Hokkaido University, Sapporo 060-0812, Japan,  
Graduate School of Environmental Earth Science, Hokkaido University, Sapporo 060-0810, Japan, and  
Max-Planck-Institut für biophysikalische Chemie, Spektroskopie und Photochemische Kinetik,  
37070 Göttingen, Germany.

Received: January 12, 2004; In Final Form: September 8, 2004

Electric-field-induced changes in the absorption, fluorescence, and phosphorescence spectra of 4-(dimethylamino)benzonitrile (DMABN) doped in a polymer film were measured, and the electric dipole moment and molecular polarizability in the locally excited (LE) and charge transfer (CT) singlet states as well as in the phosphorescent triplet state were evaluated. Time-resolved fluorescence measurements both in the absence and in the presence of electric fields were also carried out. A field-induced change in the quantum yield of the LE and CT fluorescence as well as of the phosphorescence is found and the charge transfer from the LE to the CT state is shown to be accelerated by an electric field, resulting in the field-induced decrease in the population ratio of the LE relative to the CT state. The dipole moment of the phosphorescent triplet state is found to be smaller than that of the LE state, with a value similar to that of the ground state.

## 1. Introduction

Dual fluorescence of 4-(dimethylamino)benzonitrile (DMABN) discovered by Lippert<sup>1</sup> has received considerable attention involving excitation dynamics and the properties of the emitting states. A large number of publications have appeared on steady-state fluorescence and time-resolved optical measurements of emission, absorption as well as Raman and infrared spectra.<sup>2–10</sup> It is now widely accepted that the formation of a highly polar (charge transfer) excited state via the locally excited (LE) state is essential for the appearance of dual fluorescence, and a large electric dipole moment in the excited state has been reported for the CT state.<sup>4,11</sup> Since the twisted intramolecular charge transfer (TICT) mechanism was proposed by Grabowski et al., DMABN has become well known as the representative of the so-called TICT molecules,<sup>3,12,13</sup> but a controversy still exists concerning the conformational change taking place during the reaction from the LE state to the CT state.<sup>14,15</sup> In the TICT model, a twisting of the amino group to a conformer perpendicular to the phenyl plane is considered to occur during the charge-transfer process from the LE state, which is assumed to have a coplanar configuration.<sup>2,3,12,13</sup> In a series of dual fluorescent 4-aminobenzonitriles, however, no evidence supporting the importance of a rotation of the amino group was found. This led to the introduction of the planar intramolecular charge transfer (PICT) model, in which the CT state has an essentially planarized configuration with a less-pyramidal amino nitrogen atom than in the LE state.<sup>15–20</sup> It was also pointed out in the PICT model that a small energy gap between the two lowest singlet excited states is required for the occurrence of an ICT reaction in DMABN.

When DMABN is confined in a rigid medium, which prevents a large amplitude conformational change in the amino group, an intramolecular CT process could not take place within the context of the TICT model. When the PICT model is applicable to DMABN, however, a CT process would be possible even when conformational changes are strongly restricted. In addition, according to the PICT model, the rate of the CT process should be very sensitive to shifts in the energy levels induced by an external perturbation. A control of the conformational change and an induction of the energy level shift may be brought about by applying an external electric field following the doping of a molecule into a rigid polymer film. When an electric field is applied to a molecule from the outside, two kinds of influences are expected on the absorption as well as on the emission spectra. The first influence is due to the orientation effect. Unless a molecule is fixed rigidly in a medium, it will be partially aligned because of the presence of the orientational polarizability that is induced by the interaction between the electric dipole moment and the applied electric field. The second influence is due to the intrinsic effect of the molecules and the so-called Stark shift in the energy levels taking place in the presence of electric fields, which results in a spectral shift or spectral broadening. The latter effect remains even when the molecule is rigidly fixed and cannot reorient. For DMABN in solution, both effects as well as a free conformational change may operate, but only the Stark shift may be expected when DMABN molecules are doped in a rigid polymer film. Therefore, the study of electric field effects on the optical spectra and on the dynamics of molecules doped in a rigid film is of substantial interest in the examination of the CT mechanism of DMABN. We noted that experiments on external electric field effects of DMABN doped in a polymer film offer the advantage that much higher electric fields can be applied than is possible in solution; an electric field as strong as 1 MV cm<sup>-1</sup> could be applied in

\* Corresponding author. E-mail: nohta@es.hokudai.ac.jp.

<sup>†</sup> Research Institute for Electronic Science, Hokkaido University.

<sup>‡</sup> Graduate School of Environmental Earth Science, Hokkaido University.

<sup>§</sup> Max-Planck-Institut für biophysikalische Chemie, Spektroskopie und Photochemische Kinetik.

polymer films, but the applicable field strength in solution is estimated to be  $0.2 \text{ MV cm}^{-1}$  at the highest.

In the present study, electric field effects on the absorption, fluorescence, and phosphorescence spectra of DMABN doped in a polymer film are examined under vacuum as well as under normal atmospheric conditions. On the basis of these results, the electric dipole moment and the molecular polarizability both in the Franck–Condon state prepared by optical absorption and in the excited singlet and triplet states are determined. These results are compared with those obtained in solution by using other methods, such as electrooptical emission (EOEM) or time-resolved microwave conductivity measurements (TRMC),<sup>4,11</sup> and the electric properties of the excited states of DMABN in a polymer film are discussed. Electric field effects on the photochemical processes taking place in the excited state of DMABN in PMMA are also discussed by examining the field-induced change in the quantum yield of the LE and CT fluorescence emissions as well as that of the phosphorescence. In addition, time-resolved measurements of the field-induced changes in the fluorescence decay profile of DMABN doped in a PMMA film are reported.

## 2. Experimental Section

DMABN (Aldrich) was purified by recrystallization and vacuum sublimation. Polymethyl methacrylate (PMMA, MW = 120,000, Aldrich) was purified by precipitation with a mixture of methanol and benzene followed by an extraction with hot methanol. Spectral grade benzene was used as solvent without further purification.

DMABN was dissolved in a benzene solution containing PMMA. The resulting solution was poured onto an ITO-coated quartz substrate by using the spin coating method, and the polymer films were evaporated in vacuo to completely eliminate benzene. The concentration of DMABN was in the range of 0.1 to 5 mol % in its ratio to the monomer unit of PMMA. After casting and drying the polymer film, a semi-transparent aluminum film was deposited by the vacuum vapor deposition technique. Aluminum and ITO films were used as electrodes. The thickness of the polymer films was determined by using a thickness measurement system (Nanometrics, M3000).

Optical spectra were measured both in vacuo and under atmospheric pressure at room temperature ( $\sim 293 \text{ K}$ ). Plots of the field-induced change in absorption intensity ( $\Delta A$ ) or in emission intensity ( $\Delta I_E$ ) as a function of wavelength, which are referred to as the E–A and E–E spectrum, respectively, were measured using electric field modulation spectroscopy with the same apparatus as reported previously.<sup>21,22</sup> Polarization measurements of the E–A spectra were carried out by using a Glan-Taylor prism polarizer (CASIX, PGT8210). In the emission measurements, unpolarized light was used for excitation, and unpolarized emission was detected with a propagation direction perpendicular to that of the excitation light. A sinusoidal ac voltage was applied to the samples, and the value of  $\Delta A$  or  $\Delta I_E$  was detected with a lock-in amplifier at the second harmonic of the modulation frequency. Hereafter, applied electric field is denoted by  $F$ , and its strength is represented in rms.

E–E spectra were also measured at a low temperature of 45 K in vacuo. The sample substrate was cooled using a cryogenic refrigerating system (Daikin, V202C5LR) equipped with quartz optical windows, and the temperature of the substrate was monitored using a temperature controller (Scientific Instruments, model 9600) with a silicon diode thermometer (Scientific Instruments, Si410A).

Time-resolved measurements of the fluorescence intensity in the presence and absence of  $F$  were carried out at room

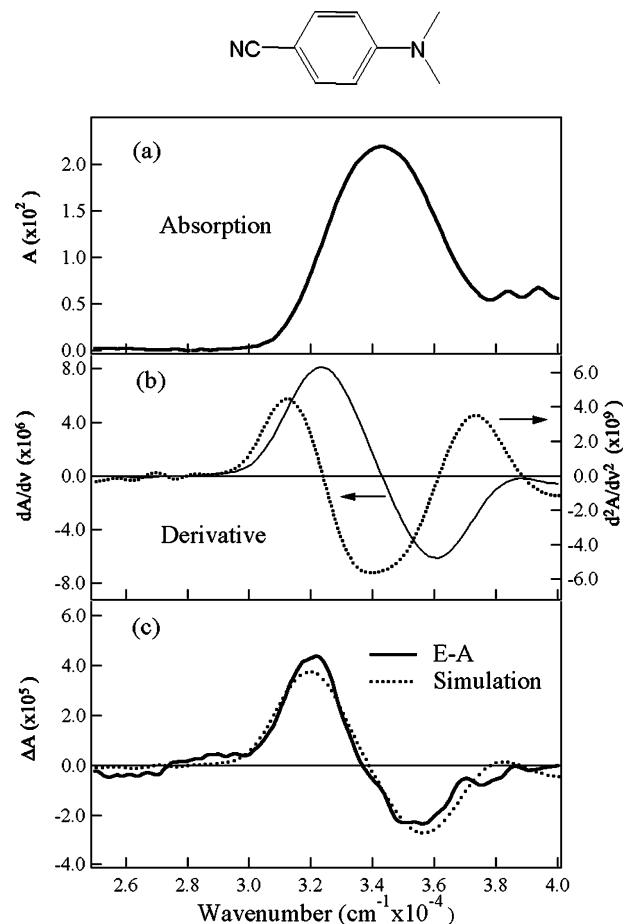


**Figure 1.** (a) Absorption spectrum of DMABN doped in a PMMA polymer film at a concentration of 0.1 mol %, (b) its first and second derivative spectra, and (c) the E–A spectrum. Applied field strength was  $0.75 \text{ MV cm}^{-1}$ . A simulation of the E–A spectrum is shown in c.

temperature by combining a single-photon counting lifetime measurement system with a homemade pulse generator supplying a bipolar square wave. The measurement system for emission decay and its field-induced change are described elsewhere.<sup>23</sup> Briefly, the emission and scattered light were detected with a microchannel plate photomultiplier (Hamamatsu R3809U-52). The excitation light source was a Ti:Sapphire laser (Tsunami, Spectra Physics) pumped by an LD laser (Millennia Xs, Spectra-Physics). The repetition rate of the laser pulse was selected to be 2 MHz with an E. O. Modulator (Model 350-160, Conoptics). The third harmonic generated by an ultrafast harmonic system (Inrad, Model 5-050) was used for excitation. The pulse width of the laser light was about 200 fs, but the actual time resolution of the decay profile is determined by the detector. The bandwidth of the instrument response function (fwhm) was  $\sim 60 \text{ ps}$  when the decay profile was measured with a time interval of 6.1 ps/channel.

## 3. Results and Discussion

**3.1. Steady-State Measurements of E–A and E–E Spectra.** Figure 1 shows the absorption and E–A spectra of DMABN doped in a PMMA polymer film at a concentration of 0.1 mol %, together with the first and the second derivatives of the absorption spectrum. The E–A spectrum was obtained at room temperature under magic angle conditions between the polarization direction of the linearly polarized excitation light and that of the applied electric field. The E–A spectra of DMABN in the region of  $25\,000\text{--}40\,000 \text{ cm}^{-1}$  can be simulated well by a

**TABLE 1: Field-Induced Change in Emission Intensity  $\Delta I_f/I_f$  with a Field Strength of  $0.75 \text{ MV cm}^{-1}$ , and Differences  $\Delta\mu$  and  $\Delta\alpha$  between Three Excited States and the Ground State for DMABN in a PMMA Polymer Film**

	$\Delta I_f/I_f$	$\Delta\mu$ (D) <sup>a</sup>	$\Delta\alpha$ ( $\text{\AA}^3$ )
E–A	$\sim 0$	3.2 (9.8)	51
E–F			
LE	$-1.4 \times 10^{-3}$	3.4 (10.0)	25
CT	$1.1 \times 10^{-3}$	6.9 (13.5)	80
T <sub>1</sub>	$-1.2 \times 10^{-4}$	$\sim 0$ (6.6)	8

<sup>a</sup> The excited-state electric dipole moment  $\mu$  determined by adopting a value of 6.6 D for the ground-state dipole moment is listed in parentheses.

linear combination of the first and second derivatives of the absorption spectrum (Figure 1).

In the presence of  $F$ , the energy levels of DMABN are shifted, depending on the electric dipole moment and molecular polarizability of the ground and excited states. As a result, the absorption spectra as well as the emission spectra are shifted. An expression for the absorption intensity in the presence of an applied electric field was derived by Liptay.<sup>24</sup> By assuming that the original isotropic distribution in rigid matrixes such as PMMA polymer films is maintained in the presence of  $F$ , the change in absorption intensity at wavenumber,  $\nu$ , in the presence of  $F$ , that is,  $\Delta A(\nu)$ , is given by the following equation<sup>24,25</sup>

$$\Delta A(\nu) = (fF)^2 \left\{ AA(\nu) + B\nu \frac{d}{d\nu} \left[ \frac{A(\nu)}{\nu} \right] + C\nu \frac{d^2}{d\nu^2} \left[ \frac{A(\nu)}{\nu} \right] \right\} \quad (1)$$

where  $f$  represents the internal field factor. The coefficient  $A$  depends on the change in transition dipole moment, and  $B$  and  $C$  are given by eqs 2 and 3

$$B = \frac{[5\Delta\bar{\alpha} + (\Delta\alpha_m - \Delta\bar{\alpha})(3 \cos^2\chi - 1)]}{10hc} \quad (2)$$

$$C = (\Delta\mu)^2 \frac{[5 + (3 \cos^2\xi - 1)(3 \cos^2\chi - 1)]}{30h^2c^2} \quad (3)$$

where  $h$  represents the Planck's constant and  $c$  is the speed of light.  $\Delta\mu$  and  $\Delta\alpha$  are the differences in electric dipole moment and polarizability tensor, respectively, between the ground (g) and excited (e) states. They are given by eq 4

$$\Delta\mu = |\Delta\mu| \quad \Delta\bar{\alpha} = \frac{1}{3} \text{Tr}(\Delta\alpha) \quad (4)$$

where  $\Delta\mu = \mu_e - \mu_g$  and  $\Delta\alpha = \alpha_e - \alpha_g$ .  $\Delta\alpha_m$  in eq 2 denotes the diagonal component of  $\Delta\alpha$  with respect to the direction of the transition dipole moment,  $\chi$  is the angle between the direction of  $F$  and the electric vector of the excitation light, and  $\xi$  is the angle between the direction of  $\Delta\mu$  and the transition dipole moment.

The magnitude of  $\Delta A$  integrated over the full spectral band relative to the total absorption intensity is nearly zero, implying that the transition dipole as well as the radiative decay rate is not noticeably influenced by  $F$ . The magnitudes of  $\Delta\mu$  and  $\Delta\alpha$  for the absorption of DMABN were determined from the first and second derivative components, respectively (Table 1). These values are practically independent of the DMABN concentration doped in the polymer film. Note that  $\chi$  in eqs 2 and 3 is taken to be  $54.7^\circ$  for the E–A spectrum shown in Figure 1. Usually, the internal field is not the same as the applied electric field because of the dielectric properties of the environment, that is,

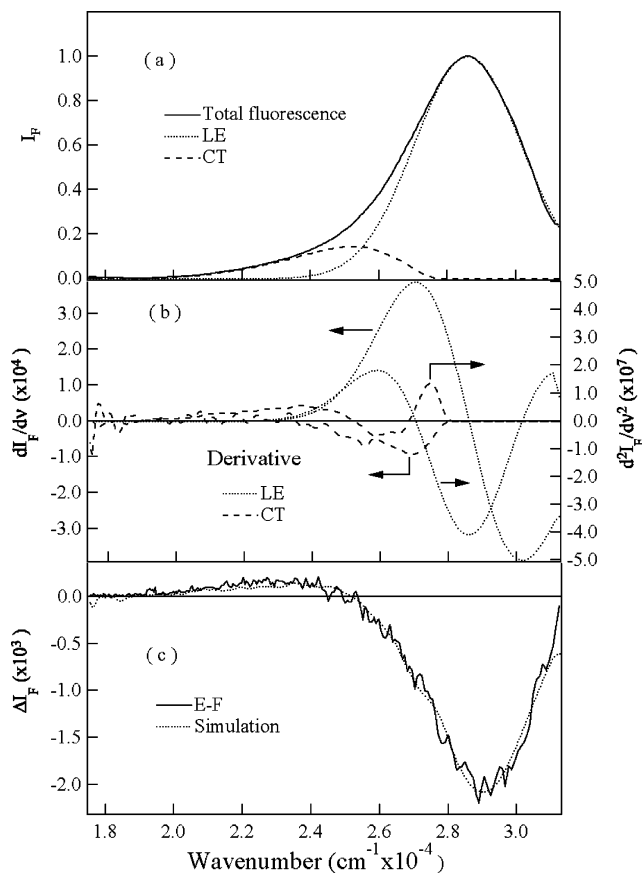


**Figure 2.** (a) Emission spectrum of DMABN doped in a PMMA polymer film at a concentration of 0.1 mol % observed at atmospheric pressure, and LE and CT fluorescence spectra, (b) the first and second derivatives of the LE and CT fluorescence spectra, and (c) the E–F spectrum. Applied field strength was  $0.75 \text{ MV cm}^{-1}$ . A simulation of the E–F spectrum is shown in c.

$f \neq 1$  in eq 1. As an appropriate approximation, the Lorentz field correction may be used for the internal field,  $f = (\epsilon + 2)/3$ , with the dielectric constant  $\epsilon$  of the material.<sup>26</sup> The dielectric constant  $\epsilon$  of PMMA is  $3.6 \pm 0.3$ ;<sup>27</sup> therefore, the internal field is about twice as large as the applied field. The magnitudes of the field-induced change in emission intensity,  $\Delta\alpha$  and  $\Delta\mu$  (Table 1), were evaluated in the present study by using the Lorentz field correction.

E–E spectra of DMABN doped in a PMMA film at a concentration of 0.1 mol % were observed with excitation at 306.5 nm, where  $\Delta A$  is negligible (Figure 1). Note that the measurements of the E–A spectra are essential not only for the evaluation of the Stark shift upon excitation but also for finding the adequate excitation wavelength for the measurements of the E–E spectra. Figures 2 and 3 show the results observed at atmospheric pressure and under vacuum conditions, respectively, at room temperature. Emission spectra in vacuo show a strong band with a peak at 441 nm, which is not observed at atmospheric pressure (Figures 2 and 3). This band is assigned to the phosphorescence of DMABN.<sup>28</sup> The phosphorescence is quenched by atmospheric oxygen (Figure 3), and a strong band at 350 nm observed at atmospheric pressure is assigned as the fluorescence of DMABN. The spectral shape of the fluorescence and phosphorescence is generally regarded to be unaffected by oxygen at atmospheric pressure, and the phosphorescence spectrum was obtained by subtracting the emission spectrum observed under atmospheric conditions from that in vacuo, normalizing on the peak at 350 nm. The E–E spectrum of the



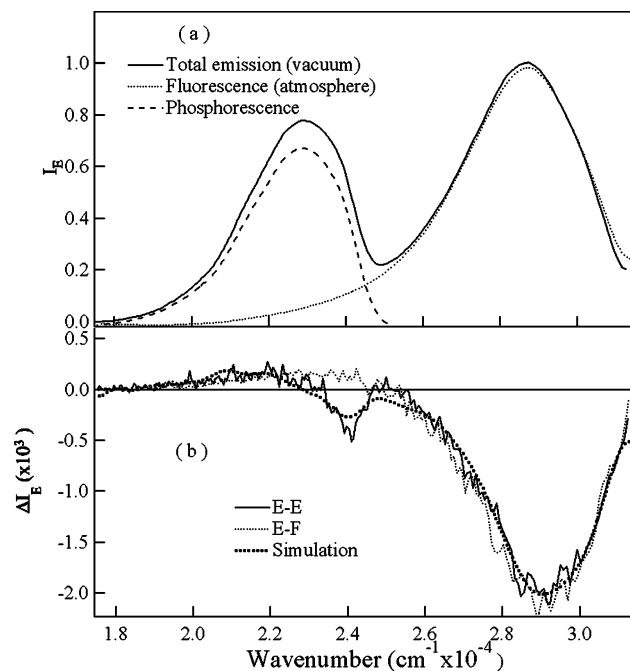


**Figure 3.** (a) Emission spectra of DMABN doped in a PMMA polymer film at a concentration of 0.1 mol % observed in vacuo (—) and under atmospheric conditions (···), and (b) the E–E and E–F spectra observed in vacuo and at atmospheric pressure, respectively. Applied field strength was  $0.75 \text{ MV cm}^{-1}$ . A simulation of the E–E spectrum is shown by a thick dotted line in b. See the text for the phosphorescence spectrum depicted in a.

phosphorescence of DMABN was similarly obtained by assuming that the E–E fluorescence spectra have an identical shape in vacuo as well as at atmospheric pressure. The results are shown in Figure 4. Hereafter, E–E spectra of fluorescence and phosphorescence are referred to as E–F and E–P spectra, respectively.

The E–F and the E–P spectra obtained at the second harmonic of the modulation frequency in a polymer film are considered to be described by an equation similar to eq 1, that is, by a linear combination of the corresponding emission spectrum and its first and second derivative spectra. The first and second derivative components correspond to the spectral shift and the spectral broadening, respectively, resulting from the difference in molecular polarizability and electric dipole moment between the emitting state and the ground state. The component of the E–F or E–P spectrum that gives the same shape as the emission spectrum corresponds to the field-induced change in emission quantum yield. Then, the observed E–F spectrum and the E–P spectrum may be simulated by a linear combination of the zeroth, first, and second derivatives of the corresponding emission spectrum.

As shown in Figure 4, the integration of the E–P spectrum of DMABN over the whole spectral region results in a negative value, indicating that the phosphorescence quantum yield decreases in the presence of  $F$ . In fact, the E–P spectrum is reproduced by a linear combination of the phosphorescence spectrum and its first derivative without including the second derivative (Figure 4). Because the C term (eq 3), which appears in the second derivative and is associated with a change in the dipole moment, is not involved in the reproduction of the E–P spectrum, we conclude that the dipole moment of the phosphorescent triplet state ( $T_1$ ) is practically the same as that of the ground state. From the first derivative part of the E–P spectra, the magnitude of  $\Delta\alpha$  between the triplet state and the ground state is estimated to be  $8 \text{ \AA}^3$  by assuming that DMABN

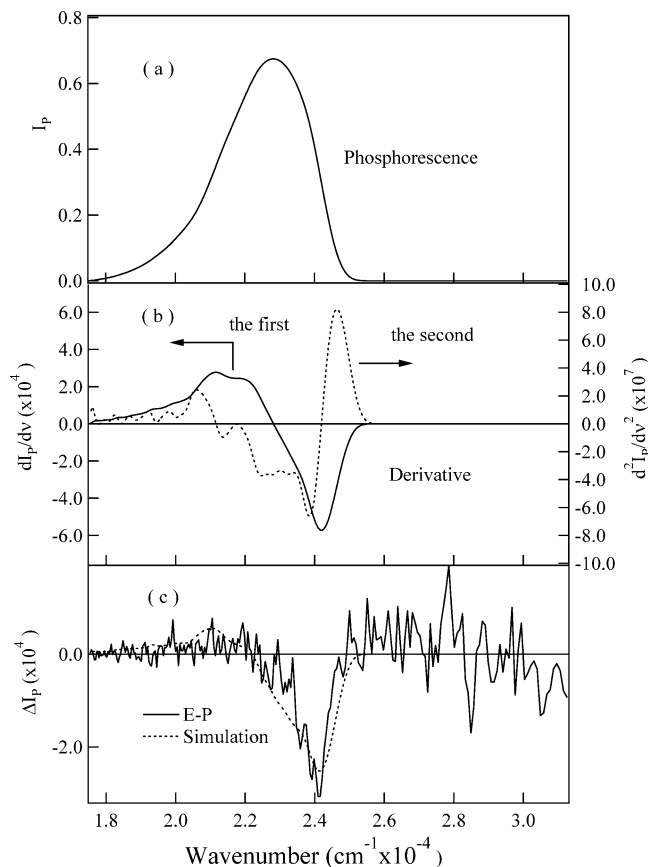


**Figure 4.** (a) Phosphorescence spectrum of DMABN doped in a PMMA film, (b) its first and second derivative spectra, and (c) the E–P spectrum. The simulated E–P spectrum is shown in c by a dotted line.

is isotropic, that is,  $\Delta\alpha_m = \Delta\bar{\alpha}$  in eq 2. The finding that the magnitude of the difference,  $\Delta\mu$ , between the  $T_1$  state and the ground state is nearly zero is an indication that the  $T_1$  state is not a CT state, which is in agreement with the results reported previously.<sup>4,5,29–31</sup> The fact that the phosphorescence quantum yield of DMABN in PMMA decreases in the presence of an electric field  $F$  implies that the  $T_1$  state is produced by intersystem crossing from the LE fluorescent state, having a population that decreases by a field-induced increase in the photoinduced intramolecular charge transfer.

We failed to reproduce an E–F spectrum by a superposition of the zeroth, first, and second derivatives of a total fluorescence spectrum (figure not shown). Remember that the emission spectrum of DMABN in a PMMA film at atmospheric environment is composed of LE and CT fluorescence spectra because the phosphorescence is quenched by oxygen.<sup>28</sup> Thus, this failure suggests that LE and CT fluorescence emissions undergo an electric field effect in a different manner. The peak at 350 nm (Figure 2a) is assigned to LE fluorescence, whereas the fluorescence from the CT state is known to be located at longer wavelengths than that of the LE state. The CT fluorescence spectrum was separated by subtracting the emission spectrum of DMABN observed in the *n*-hexane solution from that observed in the film at atmospheric pressure by normalizing the peak at 350 nm (Figure 2a). Note that the CT fluorescence of DMABN is not observed in the *n*-hexane solution.<sup>32–34</sup> The fluorescence of DMABN in this solvent shows a peak at 351 nm; therefore the spectrum was blue shifted by 1 nm for the subtraction. The resulting spectrum, which is assigned to the CT fluorescence of DMABN, has a peak at  $\sim 420 \text{ nm}$ , in

agreement with the CT fluorescence spectrum in PMMA that is reported in the literature.<sup>28</sup>

After separating the LE and CT fluorescence spectra, we have successfully reproduced a total E–F spectrum observed under atmospheric condition by a superposition of the E–F spectra of LE and CT fluorescence. Note that each E–F spectrum of LE and CT is composed of a superposition of the zeroth (Figure 2a), first, and second derivatives of LE and CT fluorescence spectra (Figure 2b). The reproduced E–F spectrum is shown in Figure 2c, together with the experimental E–F spectrum. The field-induced change in quantum yield of the LE and CT emissions was estimated from the zeroth derivative parts, and the results are presented in Table 1. The magnitudes of  $\Delta\mu$  and  $\Delta\alpha$ , resulting as a consequence of the emission process, were determined from the first and the second derivative parts of both emissions by assuming that the angle-dependent term in eqs 2 and 3 is negligible. The results are listed in Table 1. Note that these data were determined by using the Lorentz field correction.

The Stark shift that was observed in the present experiments does not provide a sign of the change in  $\Delta\mu$ , but the absolute value of the dipole moment as well as the molecular polarizability in both fluorescent states (LE and CT) may be regarded to be larger than in the ground state. The present results are compared with those obtained by other techniques. The ground-state dipole moment was reported to be 6.6 D in 1,4-dioxane.<sup>4</sup> When it is assumed that this value also holds for DMABN doped in PMMA, the electric dipole moments of DMABN in the Franck–Condon state prepared by absorption, the LE, the CT and the  $T_1$  states, are determined to be 9.8, 10.0, 13.5, and 6.6 D, respectively, in PMMA (Table 1). With the TRMC method,<sup>4</sup> the electric dipole moment of DMABN in solution was found to be 9.9, 17, and 11.9 D for the LE and CT singlet states and the lowest triplet state, respectively. The dipole moment was also reported to be 5.8 D for the LE state and 16 D for the CT state with the EOEM technique.<sup>11</sup> Invariably, the CT emitting state has a larger dipole moment than the LE emitting state, which confirms the charge-transfer character of the ICT state. The EOEM method shows that the dipole moment of the LE state is somewhat smaller than that of the ground state, whereas the dipole moment of the LE state was estimated to be 11.4 D by solvatochromism measurements.<sup>11</sup> The results reported here show that the LE state, as well as the Franck–Condon state prepared by optical absorption, has a dipole moment as large as 10 D, which shows that the LE state is strongly polar. This value is very close to the one determined from the TRMC and the solvatochromic measurements. In contrast to the fluorescent states, the dipole moment of 6.6 D found here for DMABN in the triplet state is similar to that in the ground state, implying that intersystem crossing to the triplet state from the singlet CT state is in fact a back electron transfer. The lowest triplet state is regarded to have a dipole moment smaller than that of LE. By TRMC measurements, a considerably larger dipole moment (12 D) has been reported for the triplet state of DMABN in cyclohexane and 1,4-dioxane.<sup>4</sup> The result in cyclohexane was based on a value of 0.18 for the intersystem crossing yield,  $\Phi_{isc}$ . With the recent averaged value of 0.82 determined for the  $\Phi_{isc}$  of DMABN in four alkane solvents at 25 °C,<sup>34</sup> we obtained a considerably lower dipole moment of 8.1 D for the  $T_1$  state of DMABN, much closer to the 6.6 D determined here in PMMA.

Both in vacuo and at atmospheric pressure, the quantum yield of the LE fluorescence decreases in the presence of  $F$ , which suggests that the LE  $\rightarrow$  CT charge-transfer reaction is accelerated by  $F$ . In fact, the E–E spectra at atmospheric pressure were simulated by assuming that the CT fluorescence yield is

increased by  $F$ . This field dependence is related to the solvent effect; the CT fluorescence becomes stronger as the polarity of the solvent becomes larger,<sup>35,36</sup> which implies that the application of  $F$  plays a role that is similar to an increase in the solvent polarity. The present results show that with DMABN in PMMA the CT process is still influenced by  $F$ . This is not surprising because it has been found that DMABN shows dual fluorescence in ethanol glasses below the glass transition point, which seems to provide evidence against the occurrence of a large amplitude motion such as TICT during the ICT reaction.<sup>18</sup>

Room temperature is much lower than the glass transition temperature of PMMA (387 K), so there is no doubt that the translational and rotational motion of DMABN are restricted.<sup>37,38</sup> However, the degree of restriction in PMMA, which probably depends on the size of the dopant dye and on the dye–PMMA interaction, is not known well for DMABN. A question may then arise, whether the CT process of DMABN and its electric field effect in PMMA are attributed to a molecular motion that may occur slightly in PMMA at room temperature. With respect to this problem, the temperature dependence of emission and E–E spectra seem to be very informative. Therefore, emission and E–E spectra of DMABN doped in PMMA were observed at a low temperature of 45 K in vacuo. The results are very similar to the ones observed at room temperature; LE fluorescence is quenched by  $F$ , whereas CT fluorescence is enhanced by  $F$ , irrespective of temperature. The magnitude of the field-induced change in quantum yield at 45 K is nearly the same as that at room temperature for both LE and CT emissions. A noticeable difference in emission and E–E spectra between room temperature and 45 K is that the phosphorescence intensity is slightly enhanced by lowering the temperature, and as a result, the intensity of the E–P spectrum becomes stronger at 45 K than it is at room temperature. These results seem to show clearly that a large amplitude motion such as TICT is not necessary during the ICT reaction and that ICT reaction is influenced by  $F$  as a result of the field-induced shift in energy levels.

The refractive index of the matrix (PMMA) may change in the presence of an electric field, that is, the so-called DC Kerr effect is expected.<sup>39</sup> It may be pointed out that the field-induced change in emission quantum yield results from the change in radiative decay rate constant, as a result of the field-induced change in refractive index of PMMA. Note that the radiative decay rate constant depends on the refractive index of the matrix.<sup>40</sup> To examine this field effect, we evaluated the magnitude of the DC Kerr effect for PMMA. In the presence of a static electric field, the birefringence ( $\Delta n$ ) is given as follows

$$\Delta n = \lambda B F^2 \quad (5)$$

where  $\lambda$  is light wavelength,  $B$  is the Kerr constant, and  $F$  is the applied field strength. The  $B$  value of PMMA film is reported to be  $1.5 \times 10^{-15} \text{ mV}^{-2}$ .<sup>39</sup> In the present experiments, light excitation was at around 300 nm, and the applied field strength was  $1 \text{ MV cm}^{-1}$ , that is,  $1 \times 10^8 \text{ Vm}^{-1}$ ; therefore,  $\Delta n$  is estimated to be  $4.6 \times 10^{-6}$ . The magnitude of the field-induced change in refractive index is considered to be the same order of magnitude as  $\Delta n$ . The refractive index ( $n$ ) of PMMA at 300 nm is considered to be not too different from 1.5, which is the refractive index of PMMA at around 450 nm.<sup>27</sup> Thus, the ratio of  $\Delta n/n$  (about  $\sim 3 \times 10^{-6}$ ) is several orders of magnitude smaller than the magnitude of the field-induced change in fluorescence intensity or in preexponential factor of the fluorescence decay ( $> 1 \times 10^{-3}$ ). Therefore, the change in the radia-

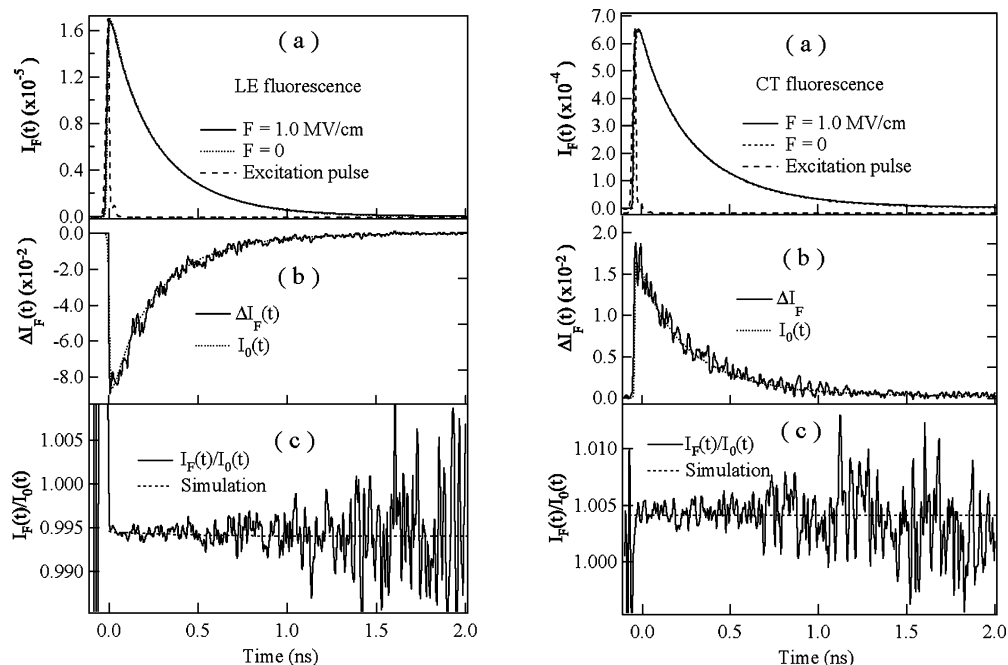


**Figure 5.** (a) Fluorescence decays of DMABN doped in a PMMA film at 0.1 mol % observed at 350 nm (left) and at 423 nm (right) at zero field (···) and in the presence of  $1.0 \text{ MV cm}^{-1}$  (—), (b) the difference  $I_F(t) - I_0(t)$  between the fluorescence decay at zero field ( $I_0(t)$ ) and the decay at  $1.0 \text{ MV cm}^{-1}$  ( $I_F(t)$ ) and the fluorescence decay at zero field (···), and (c) the ratio  $I_F(t)/I_0(t)$ . These results were obtained in atmospheric pressure with excitation at 306.5 nm. The pulse shape of the scattered light, which corresponds to the response curve of the detection system, is shown in a.

tive decay rate induced by a field-induced change in refractive index of PMMA is negligible in the present experiments.

**3.2. Time-Resolved Measurements of the Field-Induced Change in Fluorescence Decay Profile.** Direct measurements of the field-induced change in the fluorescence decay profile of DMABN in PMMA also indicate that the charge-transfer process is accelerated by an electric field. Figure 5 shows emission decays of DMABN doped in a PMMA polymer film at 0.1 mol % observed at zero field and in the presence of an electric field of  $1.0 \text{ MV cm}^{-1}$ . These decays were measured at atmospheric pressure at room temperature by monitoring the emission at 350 and 423 nm, respectively, corresponding to the LE and CT fluorescence emissions. The difference  $I_F(t) - I_0(t)$  between the decay at zero field ( $I_0(t)$ ) and that at  $1.0 \text{ MV cm}^{-1}$  ( $I_F(t)$ ), referred to as  $\Delta I_F(t)$ , and the ratio  $I_F(t)/I_0(t)$  are also shown in Figure 5.

We note that the fluorescence decays of DMABN doped in a PMMA polymer are expressed by a biexponential function,  $I_F(t) = A_1 \exp(-t/\tau_1) + A_2 \exp(-t/\tau_2)$ , as reported by Al-Hassan,<sup>41</sup> and the two decay times and their preexponential factors are shown in Table 2 for the LE and CT fluorescence emissions. When the LE and CT states are in equilibrium, the decay times  $\tau_1$  and  $\tau_2$  of both states must be the same, as shown to be the case in solution.<sup>3</sup> In contrast with the results in solution, however, the decay times of the CT fluorescence are somewhat longer than that of the LE fluorescence. As the origin of the multiexponential decays as well as of the disagreement between the LE and CT fluorescence decay times, the complex anisotropic PMMA environment may be envisaged, in which DMABN may show a variation of fluorescence properties because its fluorescence yield and decay time are known to depend on the nature of the solvent matrix. DMABN molecules in different PMMA environments may, therefore, show different decay times and different population ratios between the LE and CT states, even when the equilibrium between LE and CT states is established. As a result, the fluorescence decay times may

**TABLE 2: Decay Times  $\tau_i$  and Preexponential Factors  $A_i$  of the LE and CT Fluorescence at Atmospheric Pressure (P) and under Vacuum Conditions (V)**

		$\tau_1$ (ns)	$A_1^a$	$\tau_2$ (ns)	$A_2$
LE fluorescence					
(P)	zero field	1.67	(1)	3.47	1.519
	$1.0 \text{ MV cm}^{-1}$	1.67	0.995	3.47	1.510
(V)	zero field	1.82	(1)	3.61	2.006
	$1.0 \text{ MV cm}^{-1}$	1.79	0.986	3.58	2.004
CT fluorescence					
(P)	zero field	1.99	(1)	4.34	1.052
	$1.0 \text{ MV cm}^{-1}$	1.99	1.008	4.34	1.054

<sup>a</sup> The amplitude  $A_1$  of the fast decaying component at zero field is normalized to unity.

depend on the monitoring wavelength, as observed in the present experiments in PMMA. The validity of this assumption may be rationalized by the single molecule spectroscopy of a dye chromophore doped in a PMMA matrix investigated by Ishikawa et al.<sup>42</sup> They found that the fluorescence histogram of crystal violet (CV) shows a bimodal distribution in PMMA. On the basis of this, it was suggested that the sites in a PMMA matrix are roughly separated into two classes, namely, viscous and less-viscous sites, which causes the interaction of individual CV molecules with PMMA to be different from site to site. The biexponential fluorescence decay of DMABN observed here in PMMA seems to correspond well with the results of CV in PMMA.

The fast decaying portion of the fluorescence of DMABN, with a decay time around 20 ps at 25 °C in a 1,4-dioxane solution,<sup>4,43</sup> was not observed in a PMMA polymer film, and only the slowly decaying portion (ns region) was obtained. In agreement with the steady-state E-E spectra, the  $\Delta I_F(t)$  of the LE fluorescence at 350 nm is negative over the whole time region, showing the field-induced quenching of the LE fluorescence. The time dependence of  $\Delta I_F(t)$  is similar to the decay



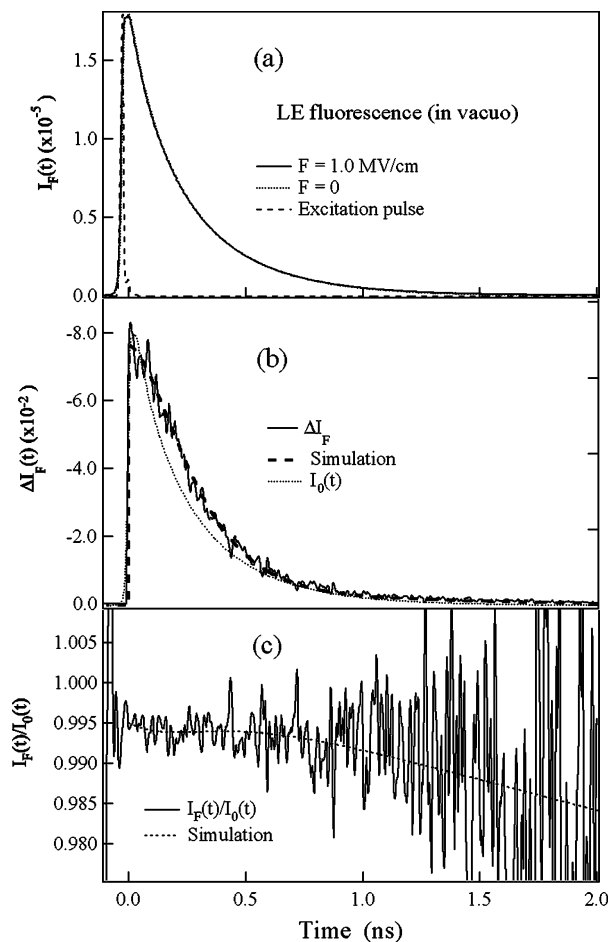


**Figure 6.** (a) Fluorescence decays of DMABN doped in a PMMA film at 0.1 mol % observed at 350 nm at zero field (···) and in the presence of 1.0 MV cm<sup>-1</sup> (—), (b) the difference  $I_F(t) - I_0(t)$  between the fluorescence decay at zero field ( $I_0(t)$ ) and the decay at 1.0 MV cm<sup>-1</sup> ( $I_F(t)$ ), and the fluorescence decay at zero field (···), and (c) the ratio  $I_F(t)/I_0(t)$ . These results were obtained in vacuo with excitation at 306.5 nm. The pulse shape of the scattered light is shown in a by a dashed line.

profile itself, indicating that the population of the fluorescent LE state, but not the fluorescence decay, is influenced by  $F$ . As a result,  $I_F(t)/I_0(t)$  is nearly constant during the entire decay for the LE as well as the CT fluorescence emission (Figure 5). In contrast to the LE fluorescence,  $\Delta I_F(t)$  of the CT fluorescence is positive over the full decay, and the time-dependence of  $\Delta I_F(t)$  is also practically identical in shape to the decay profile itself. These results indicate that the population lifetime of the LE and CT fluorescent states in equilibrium is not influenced by  $F$  and that only the population ratio between the fluorescent LE and CT states is influenced by an electric field. The field-induced population increase in the CT state and the corresponding decrease in the LE state show that the initial step of the charge transfer process from the LE to the CT state is enhanced by an electric field, as expected from the steady-state measurements of electric field effects on fluorescence, as described above. In fact, only the preexponential factors, but not the decay times, of the fluorescence are influenced by the field  $F$ , as shown in Table 2. The observed field effects on the preexponential factor implies that the rate of the initial charge-transfer step increases by a factor of 0.5–1.0% in the presence of 1 MV cm<sup>-1</sup>.

Electric field effects on the LE fluorescence decay of DMABN in PMMA were also measured under vacuum conditions at room temperature. The fluorescence decay,  $\Delta I_F(t)$  and

$I_F(t)/I_0(t)$  observed in vacuo are shown in Figure 6. The LE fluorescence shows a biexponential decay, as found at atmospheric pressure (Table 2). The lifetime and preexponential factor of each decay component are shown in Table 2. The LE fluorescence is quenched by  $F$  even at early times, which is similar to the result observed at atmospheric pressure. In contrast with these results, however, the time dependence of  $\Delta I_F(t)$  is different from that of the fluorescence decay, indicating that the fluorescence decay times are influenced by  $F$ . In fact,  $I_F(t)/I_0(t)$  is not constant over the entire decay, but decreases with increasing time. As shown in Table 2, the decay time becomes shorter and the preexponential factor becomes smaller in the presence of  $F$ . The latter is caused by the field-induced increase in the charge transfer in the reaction from the LE to the CT state, which results in a change in population of the LE and CT states. The former implies that the CT decay time becomes shorter in the presence of an electric field, when the LE and CT states are regarded as being in equilibrium. A clear interpretation can, however, at present not be given to explain why the LE fluorescence decay time is influenced by  $F$  only under vacuum conditions.

#### 4. Conclusions

Charge transfer (ICT) from the LE to the CT state occurs in DMABN doped in a polymer film of PMMA. The LE fluorescence is quenched by applying an electric field, whereas the CT fluorescence is enhanced by this field, suggesting that the ICT rate is accelerated by the application of an electric field. The similar field effects were observed both at room temperature and at a low temperature of 45 K, suggesting that a large amplitude motion is not necessary for either the ICT reaction of DMABN or its electric field dependence. Direct measurements of the fluorescence decay show that the LE/CT population ratio becomes smaller when an external electric field is applied, supporting the idea that the ICT rate is enhanced by an electric field. In the present experiments, however, the fast decaying component of the LE fluorescence, whose rate is regarded as the ICT rate, could not be defined in PMMA. A much better time resolution may be necessary in emission measurements to separate the fast component of the LE fluorescence for the direct confirmation of the field effect on the ICT rate in PMMA. The measurements of the Stark shift in the absorption, LE fluorescence, CT fluorescence, and phosphorescence spectra of DMABN in PMMA led to values for the change in polarizability ( $\Delta\alpha$ ) and electric dipole moment ( $\Delta\mu$ ) between each excited state and the ground state. The magnitude of the change,  $\Delta\mu$ , between the phosphorescent state and the ground state is very small, which means that the T<sub>1</sub> state has a smaller dipole moment than the LE state. The intersystem crossing from the LE to the triplet state can therefore be regarded as a back charge-transfer process.

**Acknowledgment.** This work was supported by Grants-in-Aid for Scientific Research (A) (2) (15205001) and by Scientific Research on Priority Area (417) from the Ministry of Education, Culture, Sports, Science, and Technology of Japan. N. O. was also supported by the Research Foundation for Opto-Science and Technology.

#### References and Notes

- (1) Lippert, E.; Lüder, W.; Boos, H. In *Advances in Molecular Spectroscopy*; Mangini, A., Ed.; Pergamon Press: Oxford, U.K., 1962; p 443.
- (2) Rotkiewicz, K.; Grellman, R. H.; Grabowski, Z. R. *Chem. Phys. Lett.* **1973**, *19*, 315. Rotkiewicz, K.; Grabowski, Z. R.; Krowczyński, A.;



- Künnle, W. *J. Lumin.* **1976**, 12/13, 877. Grabowski, Z. R.; Rotkiewicz, K.; Siemiarczuk, A.; Cowley, D. J.; Baumann W. *Nouv. J. Chim.* **1979**, 3, 443.
- (3) Leinhos, U.; Kühnle, W.; Zachariasse, K. A. *J. Phys. Chem.* **1991**, 95, 2013.
- (4) Schuddeboon, W.; Jonker, S. A.; Warman, J. M.; Leinhos, U.; Kühnle, W.; Zachariasse, K. A. *J. Phys. Chem.* **1992**, 96, 10809.
- (5) Okada, T.; Uesugi, M.; Köhler, G.; Rechthaler, K.; Rotkiewicz, K.; Rettig, W.; Grabner, G. *Chem. Phys.* **1999**, 241, 327.
- (6) Kwok, W. M.; Ma, C.; Matousek, P.; Parker, A. W.; Phillips, D.; Toner, W. T.; Towrie, M. *Chem. Phys. Lett.* **2000**, 322, 395.
- (7) Kwok, W. M.; Ma, C.; Matousek, P.; Parker, A. W.; Phillips, D.; Toner, W. T.; Towrie, M.; Umapathy, S. *J. Phys. Chem. A* **2001**, 105, 984.
- (8) Hashimoto, M.; Hamaguchi, H. *J. Phys. Chem.* **1995**, 99, 7875.
- (9) Chudoba, C.; Kummrow, A.; Dreyer, J.; Stenger, J.; Nibbering, E. T. J.; Elsaesser, T.; Zachariasse, K. A. *Chem. Phys. Lett.* **1999**, 309, 357.
- (10) Okamoto, H.; Kinoshita, M.; Kohtani, S.; Nakagaki, R.; Zachariasse, K. A. *Bull. Chem. Soc. Jpn.* **2002**, 75, 957.
- (11) Baumann, W.; Bischof, H.; Fröhling, J.-C.; Brittinger, C.; Rettig, W.; Rotkiewicz, K. *J. Photochem. Photobiol., A* **1992**, 64, 49.
- (12) Braun, D.; Rettig, W. *Chem. Phys.* **1994**, 180, 231.
- (13) Saielli, G.; Polimeni, A.; Nordio, P. L.; Bartolini, P.; Ricci, M.; Righini, R. *Chem. Phys. Lett.* **1997**, 223, 51.
- (14) Rettig, W.; Bliss, B.; Dirnberger, K. *Chem. Phys. Lett.* **1999**, 305, 8.
- (15) Zachariasse, K. A. *Chem. Phys. Lett.* **2000**, 320, 8.
- (16) Zachariasse, K. A.; von der Haar, M. G. Th.; Hebecker, A.; Il'ichev, Yu. V.; Jiang, Y.-B. *J. Photochem. Photobiol., A* **1996**, 102, 59.
- (17) Il'ichev, Y. V.; Kühnle, W.; Zachariasse, K. A. *J. Phys. Chem. A* **1998**, 102, 5670.
- (18) Demeter, A.; Druzhinin, S.; George, M.; Haselbach, E.; Roulin, J.-L.; Zachariasse, K. A. *Chem. Phys. Lett.* **2000**, 323, 351.
- (19) Zachariasse, K. A.; Druzhinin, S. I.; Bosch, W.; Machinek, R. *J. Am. Chem. Soc.* **2004**, 126, 1705.
- (20) Techert, S.; Zachariasse, K. A. *J. Am. Chem. Soc.* **2004**, 126, 5593.
- (21) Umeuchi, S.; Nishimura, Y.; Yamazaki, I.; Murakami, H.; Yamashita M.; Ohta, N. *Thin Solid Films* **1997**, 311, 239.
- (22) Ohta, N.; Koizumi, M.; Umeuchi, S.; Nishimura, Y.; Yamazaki, I. *J. Phys. Chem.* **1996**, 100, 16466.
- (23) Tsushima, M.; Ushizaka, T.; Ohta, N. *Rev. Sci. Instrum.* **2004**, 75, 479.
- (24) Liptay, W. In *Excited States*; Lim, E. C., Ed.; Academic Press: New York, 1974; Vol. 4, p 129.
- (25) Bublitz, G. U.; Boxer, S. G. *Annu. Rev. Phys. Chem.* **1997**, 48, 213.
- (26) Böttcher, C. J. F.; Bordewijk, P. *Theory of Electric Polarization*; Elsevier: Amsterdam, 1978; Vol. 1.
- (27) *Polymer Handbook*; Brandrup, J., Immergut, E. H., Eds.; John Wiley & Sons: New York, 1975.
- (28) Lang, J. M.; Dreger, Z. A.; Drickamer, H. D. *J. Phys. Chem.* **1994**, 98, 11308.
- (29) Köhler, G.; Grabner, G.; Rotkiewicz, K. *Chem. Phys.* **1993**, 173, 275.
- (30) Chattopadhyay, N.; van der Auweraer, M.; De Schryver, F. C. *Chem. Phys. Lett.* **1997**, 279, 303.
- (31) Chattopadhyay, N.; Romments, J.; van der Auweraer, M.; De Schryver, F. C. *Chem. Phys. Lett.* **1997**, 264, 265.
- (32) Lippert, E.; Lüder, W.; Moll, F.; Nägele, W.; Boos, H.; Prigge, H.; Seibold-Blankenstein, I. *Angew. Chem.* **1961**, 73, 695.
- (33) Rettig, W. *Angew. Chem., Int. Ed. Engl.* **1986**, 25, 971.
- (34) Druzhinin, S. I.; Demeter, A.; Galievsky, V. A.; Yoshihara, T.; Zachariasse, K. A. *J. Phys. Chem. A* **2003**, 107, 8075.
- (35) Hicks, M.; Vandersall, M. T.; Sitzmann, E. V.; Eisenthal, E. B. *Chem. Phys. Lett.* **1987**, 135, 413.
- (36) Kosower, E. M.; Dodiuk, H. *J. Am. Chem. Soc.* **1976**, 98, 924.
- (37) Chowdhury, A.; Locknar, S. A.; Premvardhan, L. L.; Peteanu, L. A. *J. Phys. Chem. A* **1999**, 103, 9614.
- (38) Deschenes, L. A.; Banden Bout, D. A. *J. Phys. Chem. B* **2001**, 105, 11978.
- (39) Hartig, C.; Kleppinger, R.; Jungnickel, B.-J. *Polymer* **1995**, 36, 4553.
- (40) Strickler, S. J.; Berg, R. A. *J. Chem. Phys.* **1962**, 37, 814.
- (41) Al-Hassan, K. A. *J. Polymer Sci., Part B: Polym. Phys.* **1995**, 33, 725.
- (42) Ishikawa, M.; Ye, J. Y.; Maruyama, Y.; Nakatsuka, H. *J. Phys. Chem. A* **1999**, 103, 4319.
- (43) Zachariasse, K. A.; Yoshihara, T.; Druzhinin, S. I. *J. Phys. Chem. A* **2002**, 106, 6325.